International Journal of Heat and Mass Transfer 52 (2009) 4650–4658

Contents lists available at ScienceDirect

International Journal of Heat and Mass Transfer

journal homepage: www.elsevier.com/locate/ijhmt

Experimental study on the effect of heat transfer enhancement devices in flat-plate solar collectors

Alireza Hobbi [a], Kamran Siddiqui [a,b,*]

[a] Department of Mechanical and Industrial Engineering, Concordia University, Montreal, Canada H3G 1M8
[b] Department of Mechanical and Materials Engineering, University of Western Ontario, London, Canada N6A 5B9

ARTICLE INFO

Article history:
Received 5 June 2008
Received in revised form 3 March 2009
Available online 4 May 2009

Keywords:
Flat-plate collectors
Heat transfer enhancement devices
Mixed convection

ABSTRACT

We report on an experimental study conducted to investigate the impact of heat enhancement devices on the thermal performance of a flat-plate solar collector. Different passive heat enhancement devices that include twisted strip, coil-spring wire and conical ridges were studied. The comparison showed no appreciable difference in the heat flux to the collector fluid. A detailed investigation of the observed trend showed significantly high values of Grashof, Richardson and Rayleigh numbers indicating that the heat transfer mode in the solar collector is of mixed convection type with free convection as the predominant mode. It is concluded that due to the significant damping of shear-produced turbulence by buoyancy forces, the applied passive methods based on the enhancement of shear-produced turbulence are ineffective in augmenting heat transfer to the collector fluid in flat-plate solar collectors.

1. Introduction

One of the major shortcomings of flat-plate solar collectors in cold climate is high thermal losses from the absorber plate to the surrounding, which causes the reduction of the useful energy gain, which in turn, reduces the collector efficiency. The useful energy gain, q'_u, is defined as:

$$q'_u = WF'[S - U_L(T_f - T_{amb})] \quad (1)$$

where F' is the collector efficiency factor expressed as [1]

$$F' = \frac{1/U_L}{W\left[\frac{1}{U_L[D+(W-D)F}+\frac{1}{C_B}+\frac{1}{\pi D_i h_{f,i}}\right]} \quad (2)$$

Several methods have been studied to suppress thermal and radiative losses from flat-plate solar collectors [1]. Most of these studies are focused on insulating the collector box, applying special coats on the absorber plate, using multiple cover glazes, inserting transparent insulation material between the absorber plate and the glaze, evacuating the gap between the glaze and plate, and applying antireflective coats on the glaze. Alternatively, by increasing F', the useful energy increases which compensates for the thermal losses to the surroundings. In addition, an increase in useful energy results in a cooler plate that lowers the heat loss from the plate to the surroundings. Eq. (2) shows that for the given loss coefficient (U_L), bond conductance (C_B) and tube diameter and spacing, F' can be increased by increasing the heat transfer coefficient ($h_{f,i}$) inside the tube. That is, heat transfer augmentation to the collector fluid. An enhancement of heat transfer rate in solar collectors would have a significant impact on the overall performance of the solar water heating systems. Duffie and Beckman [1] suggested that an increase in $h_{f,i}$ from 100–300 W/m^2 K for laminar flows, and 1000 W/m^2 K and above for turbulent flows results in a significant improvement in the performance of solar energy systems.

Enhancement of heat transfer rate between the pipe wall and flow during forced convection has been studied extensively over the past few decades. Different passive heat enhancement techniques have been developed and employed in a variety of applications. Passive techniques such as extending or coating the heat transfer surfaces, using various devices to generate swirl or vortices in the flow, adding projections in the inner surface of the pipe to increase the roughness, inserting helical ridges and/or grooves into the inner surface of pipe, or twisting the pipe itself, have been shown as very successful techniques. Most of the passive methods are used to increase the heat transfer coefficient by disrupting the thermal boundary layer, increasing the effective Reynolds number, or increasing the temperature and velocity gradients. Enhancement of heat transfer rate by a passive method, however, is associated with additional frictional and pressure losses due to secondary flows.

The passive heat enhancement techniques have been widely studied in forced convection applications. Smithberg and Landis [2] studied heat transfer characteristics, velocity distribution and frictional losses in a fully developed turbulent flow inside a pipe with twisted strip turbulators, under isothermal and forced

* Corresponding author. Address: Department of Mechanical and Materials Engineering, University of Western Ontario, London, Canada N6A 5B9. Tel.: +1 519 661 2111x88234; fax: +1 519 661 3020.
E-mail address: ksiddiqui@eng.uwo.ca (K. Siddiqui).

0017-9310/$ - see front matter © 2009 Elsevier Ltd. All rights reserved.
doi:10.1016/j.ijheatmasstransfer.2009.03.018

Nomenclature

A_c	collector area (m^2)
C_B	collector's bond conductance (h m^2 K/kJ)
c_p	specific heat of fluid (kJ/kg °C)
T_{amb}	ambient temperature (°C)
$T_{p,m}$	mean absorber plate temperature (°C)
$T_{f,in}$	inlet fluid temperature (°C)
$T_{f,out}$	outlet fluid temperature (°C)
$T_{f,avg}$	average bulk water temperature (°C)
T_{ph}	panel heater's surface temperature (°C)
$T_{f,b}$	bulk fluid temperature (°C)
T_w	pipe wall temperature (°C)
D_i	inside diameter of the pipe (m)
F'	collector efficiency factor
Gr	Grashof number
Gr_q	modified Grashof number
$h_{f,i}$	heat transfer coefficient between the pipe wall and the circulating fluid (W/m^2 °C)
I_T	solar radiation incident on the collector surface per unit area (W/m^2)
k	thermal conductivity (W/m^2 °C)
k_f	fluid thermal conductivity (W/m^2 °C)
l	collector length (m)
L	pipe length (m)
$\dot{m}$	flow rate (kg/s)
Nu	Nusselt number
Pr	Prandtl number
Re	Reynolds number
Ra	Rayleigh number
Ra_q	modified gradient Rayleigh number
Ri	Richardson number
Ri_q	modified Richardson number
S	daily or monthly absorbed solar energy by the collector (MJ/m^2)
t	thickness (m)
q_l	average heat transfer rate per unit length (W/m^3)
q_u	useful energy gain per area (W/m^2)
q_w	average pipe wall heat flux (W/m^2)
Q_u	useful energy (W)
U	axial flow velocity (m/s)
U_L	collector overall heat loss coefficient (W/m^2 °C)
W	collector's tube spacing (m)
ρ	density of the fluid (kg/m^3)
η	collector efficiency
δ_p	absorber plate thickness (m)
θ	dimensionless temperature
Δ	difference
ν	kinematic viscosity (m^2/s)
β	thermal expansion coefficient (°C^{-1})

convection conditions. They recommended twisted tapes as inexpensive but effective way to increase Nusselt number in heat exchangers. Narezhnyy and Sudarev [3] studied the effect of a helical bent turbulator placed at the pipe inlet, and found that the increase in pressure drop was not as significant as the enhancement of heat transfer rate. Hong and Bergles [4] experimentally determined the heat transfer coefficient of electrically heated tube with two twisted strips. For a fully developed laminar flow, they found that the Nusselt number is nine times larger than that of a tube without turbulators under similar heating conditions. Junkhan et al. [5] experimentally studied the effect of different turbulators installed at the tube inlet of a fire tube boiler, and observed considerable increase in heat transferred to water. Yildiz et al. [6] studied the effect of a twisted strip profile used as the turbulator inside a concentric double-pipe heat exchanger. They reported 100% increase in the Nusselt number and stated that the rate of heat transfer can be increased further by increasing pitch number of the twists. Durmuş et al. [7] used a snail at the inlet of the inner pipe of a concentric double pipe heat exchanger to generate swirling flow and found significant increase in the Nusselt number. Promvonge and Eiamsa-ard [8] studied the impact of a snail as the swirl flow generator at the tube inlet, and conical nozzles with different pitch arrangements inside the pipe as reverse flow generators. They found that the snail and conical nozzles increased the heat transfer rate by 278% and 206%, respectively.

In all of the above-mentioned studies, where the geometry of the tested sections was basically a straight pipe, the heat transfer enhancement was achieved by modifying the flow or surface geometry. Moreover, the test pipe was subjected to a uniform heat flux or constant wall temperature that was attained by means of electrical heater wrapped around the pipe, or hot water flowing around the tube. The flat-plate collectors, on the other hand, have pipe-and-fin geometry, and the heat transfer mode to the collector is mainly due to radiation. In addition, the majority of the radiant heat flux in the form of direct radiation is incident on one side of the pipe–fin geometry. Due to this particular geometry and the heat transfer modes, neither the heat flux nor wall temperature is uniform. Thus, the results from those previous studies cannot be applied directly to a solar collector. Furthermore, since the solar irradiance that warms water is limited or low, the flow rates in solar collectors need to be kept very small (about 0.001–0.014 kg/s/m^2) in order to warm water from inlet to the desired outlet temperature. These flow rates are typically much less than the range of flow rates studied in the literature. There have been very few studies that investigated heat transfer in the tube of flat-plate solar collectors. Iqbal [9] studied heat transfer in inclined tubes. In his setup, no plates were attached to the tubes and uniform heat flux at the tube wall was provided through electrical wires coiled around the tubes. Barozzi et al. [10] considered a plate-and-tube geometry; however, the heat was supplied through equally spaced electrical wires inserted into the two plates. Ouzzane and Galanis [11] numerically analysed heat transfer in a tube with a longitudinal fin. This system is modelled as a flat-plate collector. The heat flux (solar radiation) was incident on the top surface. The bottom surface was insulated. Their results show that most of the energy is conducted to the fluid in the bottom half of the tube. They concluded that far downstream, the top half behaves as if it was under an isothermal condition. The present study is aimed at conducting a detailed experimental investigation of the effect of different passive heat transfer enhancement techniques inside flat-plate solar collectors over a range of flow rates.

2. Experimental setup and procedure

Since the main purpose of this study was to investigate the influence of heat enhancement devices on the thermal performance of the solar collector, the experiments were conducted in an indoor facility to maintain similar heat flux conditions for each experimental run. Radiant heat flux was applied to the upper side of the collector that is similar to the real application. The schematic of the experimental setup is depicted in Fig. 1. The main features of the experimental setup and instrumentation are summarized below:

Single-tube flat-plate solar collector: Test model was a flat-plate collector with a total area of 0.145 m^2. The collector was made

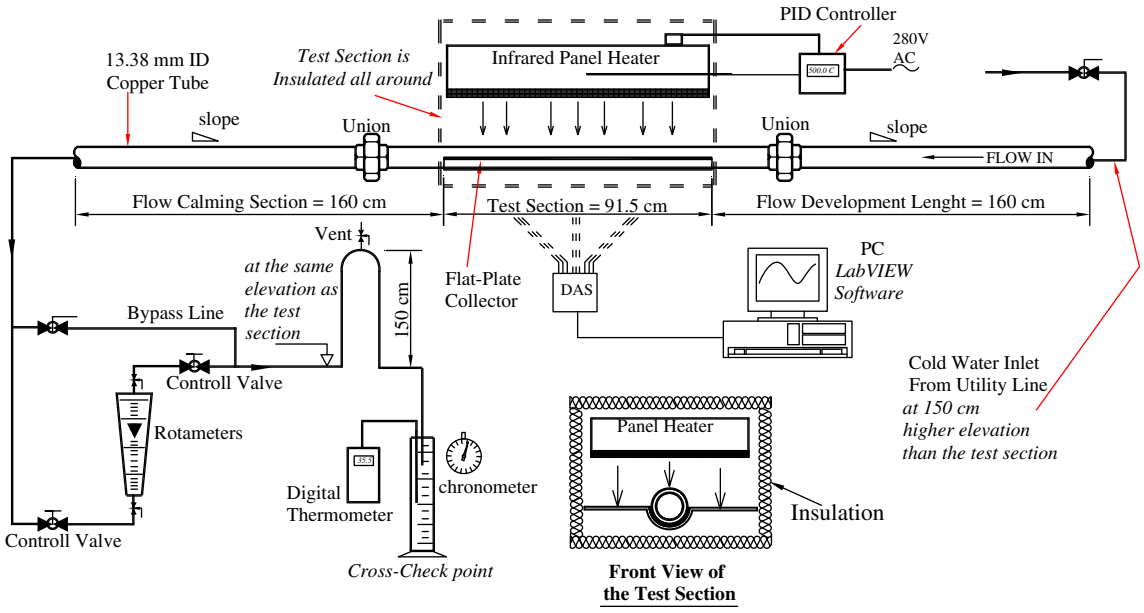

Fig. 1. Schematic of the experimental setup and instrumentation.

of 1.1 mm thick copper plate and ½″ type K commercial copper tube (ID = 13.38 mm, OD = 15.88 mm [12]). The test section of the collector was 915 mm long (see Fig. 2). The copper plate was pressed to form a groove. The copper tube was then placed in the groove and soldered to the plate by lead. The angle of contact between the tube and the groove was 130°. The entire collector was painted with high temperature black matt color.

Pannel heater: To supply thermal energy to the test section by means of radiation, a high temperature infrared panel heater (Omega QF-063610-T) was used. The heater was 2160 W at 240 V and had same dimensions as the collector (i.e. 915 × 152 mm). It was installed above and parallel to the collector. The distance from the face of the collector to the face of the heater was set equal to 50 mm. The heater has the maximum heat flux of 15,500 W/m^2 with the output wavelengths between 2.5 and 6 μm.

PID controller: To keep the heater at constant temperature an autotune PID temperature controller (Micro Omega CN77000) was used. The input temperature to the controller was taken from the center of the heater using a K type Chromega–Alomega thermocouple with ±0.4 °C accuracy. Controller has the accuracy of ±0.5 °C.

Data acquisition system: To collect the plate, tube, ambient, and water inlet and outlet temperatures, a 16 channel data acquisition card (PCI-6063-E National Instrument) was used. The card was installed in a PC and data were acquired at a rate of 100 Hz, using LabView 7 Express software.

Entrance and exit pipe lengths: To ensure that the flow was fully developed before entering the test section and it was also calm while leaving the test section, two ½″ straight copper tubes 1600 mm long were installed on both sides of the test section.

Rotameter: A rotameter was installed at the outlet of the exit pipe to measure the flow rate. Since the flow rates were very small, it was found that the installation of rotameter at the outlet of the test section minimized fluctuations in the flow rate from the set point. Control and shutdown valves were installed before and after the rotameter. To cover the entire range of flow rates studied, two variable area high accuracy rotameters were used; one (Omega FL-1448-G) in the range of 4.5–577 ml/min and the other (Omega FL-1502-A) in the range of 548–5488 ml/min.

Thermal insulation: Thermal insulation (Reflectix R-4) with radiation reflective surfaces was used to insulate the test section in order to reduce thermal and radiative losses (Fig. 1).

Thermocouples: Thermocouples were type "T" copper–constantan with the accuracy of ±0.1 °C. The thermocouples were calibrated before beginning the experiments. Thermocouples were connected onto the backside of the plate, as well as the top and bottom of the tube at three locations (i.e. the center of the test section and 50 mm from the upstream and downstream ends of the test section) using heat-transfer glues and covered with layers of duct tapes. For the thermocouples measuring the temperature at the top of the tube, a copper clip was also placed above the duct tape. Thermocouples were also inserted into the tube 5 mm upstream and downstream of the test section, respectively, to measure the change in water temperature inside the collector. The tube wall temperatures were measured for Model 1 only. The locations of the thermocouples are shown in Fig. 2.

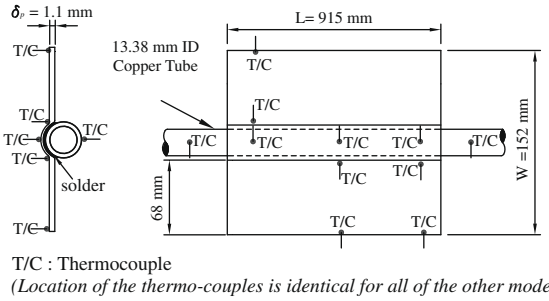

Fig. 2. Solar collector model and locations of the thermocouples.

In real applications, the solar collectors are faced south and tilted with an angle equal to 10–15° from the latitude in order to obtain maximum annual solar energy [1], which is uniform over the entire plate–tube surface exposed to the sun. In the present setup, the heater and collector were placed parallel to each other to have the uniform heat flux over the collector surface, which is

similar to the real situation. However, due to experimental reasons, they were placed horizontally. This is not expected to have a significant impact as the present study is focused on the relative comparisons of different heat augmentation approaches under the same orientation of heater and collector.

To investigate the effect of passive heat transfer augmentation methods in flat-plate solar collectors, two solar collector prototypes were designed, constructed, and used in four tested configurations (i.e. models). The description of each model is given below.

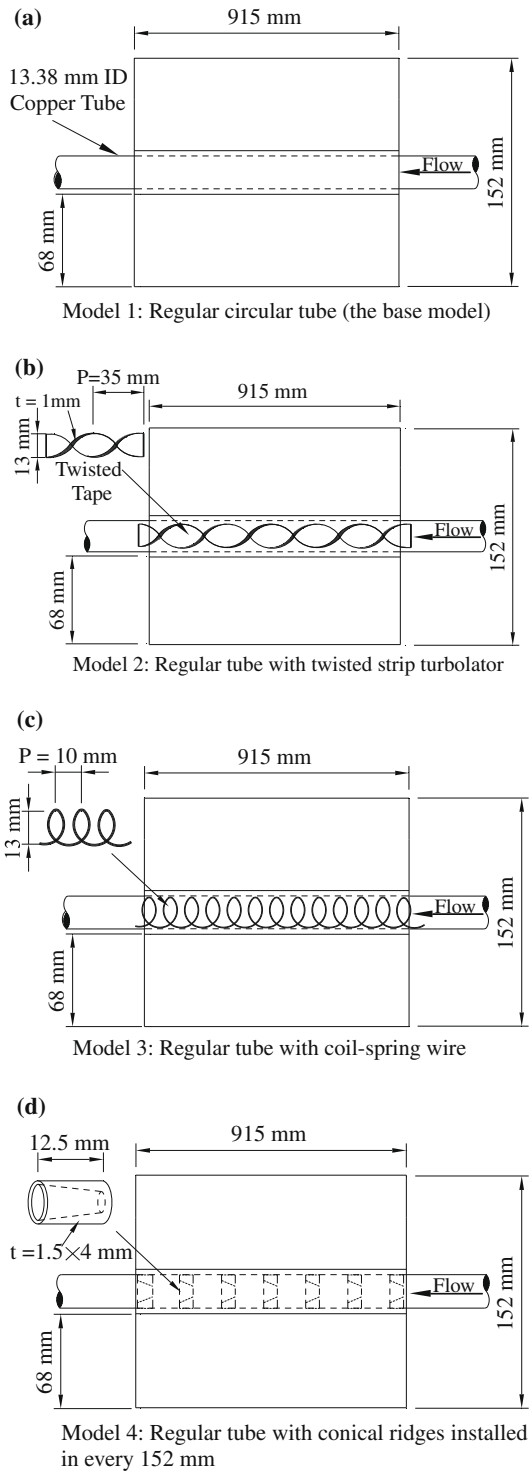

Fig. 3. Solar collector models, base and with different heat enhancement devices.

Model 1: It is the basic model, which is being used in all conventional solar water heating system with flat-plate collector. It consisted of a circular copper tube and a copper plate (fin) connected to the plate as shown in Fig. 3a. This model was used to obtain the reference data.

Model 2: In this configuration a twisted strip was inserted inside the collector tube to induce swirl flow. The twisted strip was made of 1 mm thick copper plate, and was twisted in such a way that it fits the inner diameter of the tube. Two lengths of the twisted strips were considered, one short length (25% of the test section length) and the other full length (i.e. 100% of the test section length). The detailed sketch of the model is shown in Fig. 3b. The experimental results for 25% long twisted tape were similar to 100% long and therefore, are not presented in this paper.

Model 3: In this configuration, a coli-spring wire made of copper was inserted inside the collector's tube to introduce a helical surface roughness. Both short and full lengths coils have been tested. Due to the similar results for both cases, the results for short coil are not presented here. The detailed sketch of the model is shown in Fig. 3c.

Model 4: In this configuration, conical shape ridges (diverging nozzles) made of brass were installed every 152 mm to generate longitudinal vortices inside the tube. The detailed sketch of the model is shown in Fig. 3d.

Note that for Models 2 and 3, the twisted tape and helical wires, respectively, were inserted alternatively in the same tube as for Model 1. Each model was tested for two different panel heater surface set temperatures (T_{ph}) equal to 400 and 300 °C, and for various flow rates varied from 0.132 to 1.1 l/min. The Reynolds number (based on the fluid properties at the average water temperature inside the collector) varied between 350–1900 and 280–1060 for 400 and 300 °C heater set temperatures, respectively. It was estimated that for these heater set temperatures and with 50 mm gap between the model and heater, the average absorber plate temperature is comparable with those obtained during the field test with incident solar radiation. The flow rate of 0.132 l/min (about 54 kg/h/m^2 of collector area) is close to the typical flow rates in either thermosyphon (natural) or forced (indirect) circulation flat-plate solar water collectors [13].

City water was supplied through an open circuit into the test section. The city water temperature was varied from 7 to 20 °C depending on the day of the year, but was almost constant during the data-acquisition period for a given run. Every day before starting the experiments, the system ran with the maximum flow to discharge trapped air from the system. System was also installed with slight slope towards the inlet to facilitate air removal from the system. Moreover, to ensure that the test section along with entrance and exit pipes are completely full of water during the experiments, the entire system was placed at an elevation 1500 mm lower than the water supply line and discharge point of the system (see Fig. 1). For each experimental run, the data acquisition was started 15 min after initiating the flow rate and T_{ph} to ensure steady conditions were achieved. The data were acquired for 10 min at a sampling rate of 100 Hz. Each run was repeated twice at different periods of time to ensure the experimental repeatability.

A large number of preliminary tests were conducted to optimize the experimental setup prior to the actual experimental runs. For instance, test section with or without insulation, test section with or without extra straight pipes for flow development, and flow meter installation upstream or downstream of the test section. It was found that the test section with insulation, developed flow, and flow meter located at the exit of the test section, yield steadier conditions and consistency in the measured data.

3. Data reduction

The average temperatures were obtained by time-averaging 10 min of data at each run. All properties of water were calculated at the average bulk water temperature, $T_{f,avg}$, computed as

$$T_{f,avg} = (T_{f,out} + T_{f,in})/2 \tag{3}$$

The average pipe wall, plate tip, and plate base temperatures were obtained by averaging the corresponding temperatures at three axial locations (see Fig. 2). Moreover, as mentioned earlier, each run was repeated twice and the average values based on both repeated runs for each case are presented hereinafter. Following [10], the average heat transfer rate (i.e. the energy input to the fluid) per unit length of the tested models was calculated based on the overall enthalpy increase of water inside the tube as

$$q_l = \dot{m}c_p(T_{f,out} - T_{f,in})/L \tag{4}$$

The average wall heat flux was approximated as

$$q_w = q_l/(\pi D_i) \tag{5}$$

Since the inlet water temperature varied from test to test, all temperature values were normalized to supersede the effect of inlet water temperature variations. Following [14,15], the normalized temperature is given as

$$\theta = \frac{T - T_{f,in}}{q_l/(\pi k_f)} \tag{6}$$

It was found that the absolute values of outlet, plate, and tube temperatures are function of the inlet water temperature, but the increase in the water temperature ($\Delta T_f = T_{f,out} - T_{f,in}$) is a weak function of the inlet water temperature. That is, for a given flow rate and heater set temperature, the increase in water temperature was almost the same for different inlet water temperatures. Following [10,16], the values of the local and mean Nusselt numbers are calculated as

$$Nu_x = (q_w D_i)/(T_w - T_{f,b})k_f \tag{7}$$

and

$$Nu_m = (1/x)\int_0^x Nu_x\,dx \tag{8}$$

where $T_{f,b}$ is the local bulk fluid temperature computed as

$$T_{f,b} = T_{f,in} + (q_l \cdot x)/(\dot{m}c_p) \tag{9}$$

The dimensionless parameters used in this study are computed as [17]

$$\text{Reynolds number}: \quad Re = UD/\nu \tag{10}$$

$$\text{Grashof number}: \quad Gr = g\beta D^3(T_w - T_{f,b})/\nu^2 \tag{11}$$

$$\text{Prandtl number}: \quad Pr = \nu/\alpha \tag{12}$$

$$\text{Rayleigh number}: \quad Ra = GrPr \tag{13}$$

$$\text{Richardson number}: \quad Ri = Gr/Re^2 \tag{14}$$

Following [18,10], the modified form of the Grashof number, based on the supplied heat flux is expressed as

$$Gr_q = (g\beta D_i^4 q_w)/(\nu^2 k_f) \tag{15}$$

The modified Rayleigh and Richardson numbers based on Gr_q are obtained as

$$Ra_q = Gr_q Pr \tag{16}$$

$$Ri_q = Gr_q/Re^2 \tag{17}$$

Following [19], the Richardson number in terms of the supplied heat flux in the axial direction (i.e. the flow direction) is computed as

$$Ri = (g\beta L\Delta T_f)/U^2 \tag{18}$$

4. Results and discussion

The temperature rise of water (ΔT_f) is plotted versus the mass flow rate ($\dot{m}$) for all models, and for both heater set temperature, i.e. T_{ph} = 400 and 300 °C, in Fig. 4. For both T_{ph} (i.e. incident heat fluxes), ΔT_f increases with a decrease in the mass flow rate, as expected. It can be seen that for the lowest flow rate of 2.2 g/s (0.132 l/min) the water temperature rise is between 50 and 55 °C when the heater was set at 400 °C. These values are comparable with the actual values that can be achieved with this type of collectors in summer [13]. These results also indicate that for a given T_{ph} and flow rate, ΔT_f is almost equal for all studied models. The temperature rise of water in the non-dimension form ($\Delta\theta_f$) is presented in Fig. 5 versus the Reynolds number for both T_{ph} conditions. The results show that the trend of water temperature rise in the collector is almost independent of the inlet water temperature and the heat flux.

Fig. 6 shows the average wall heat flux into the fluid (q_w) versus the mass flow rate for all models, and for both T_{ph} conditions. The results show an increase in the average wall heat flux with the flow rate. However, for given flow rate and T_{ph}, the heat flux is almost similar for all models indicating that contrary to our expectations, the application of these passive methods does not have a significant effect on the enhancement of heat transfer rate in the studied range.

The variation in the dimensionless average plate base temperatures ($\theta_{avg\text{-}base}$) and the dimensionless average plate tip temperatures ($\theta_{avg\text{-}tip}$) as a function of Reynolds number are presented in Figs. 7 and 8, respectively, for both T_{ph}. These results show that the average base and tip temperatures of the absorber plate decrease with an increase in the Reynolds number. This is because the heat removal from the system increases with the flow rate (see Fig. 6), which causes a reduction in the plate temperature. As T_{ph} is fixed for a given case, a decrease in the plate temperature results in an increase in the incident radiation heat flux, which also contributes to the increase in the wall heat flux. The results also show that for given flow rate and T_{ph}, the average base and tip temperatures are almost equal for all models.

The results in previous figures show that for a given flow rate and T_{ph}, the wall heat flux and plate temperatures are almost identical for all models. That is, for the given conditions, the heat enhancement devices used in models 2, 3, and 4 are ineffective. The purpose of heat enhancement devices is to enhance turbulence,

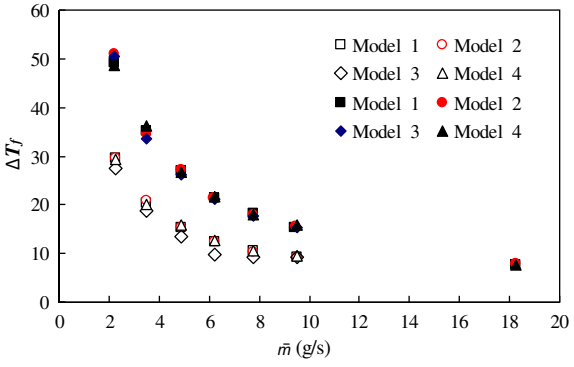

Fig. 4. Temperature rise of the water (°C) versus mass flow rate (g/s) for heater set temperatures of 400 °C (*solid symbols*) and of 300 °C (*open symbols*).

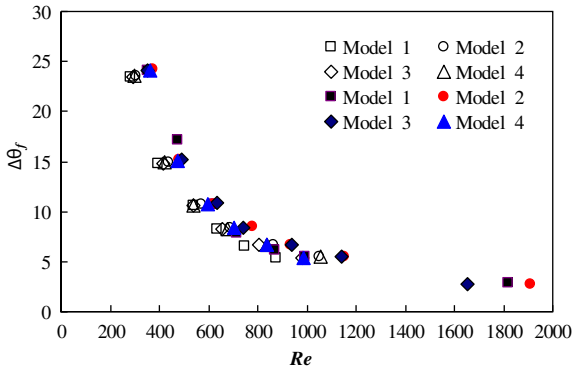

Fig. 5. Dimensionless temperature rise of the water (°C) versus Reynolds number for heater set temperatures of 400 °C (*solid symbols*) and of 300 °C (*open symbols*).

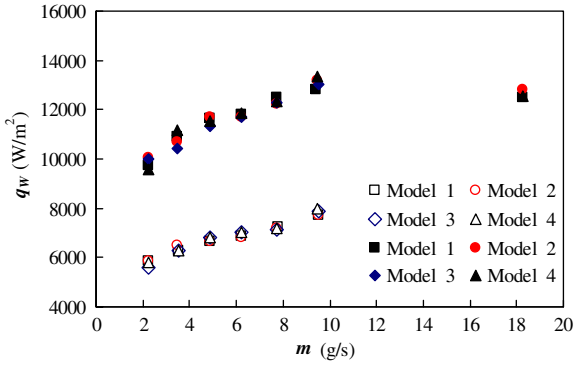

Fig. 6. Average wall heat flux (W/m^2) versus mass flow rate (g/s) for heater set temperatures of 400 °C (*solid symbols*) and of 300 °C (*open symbols*).

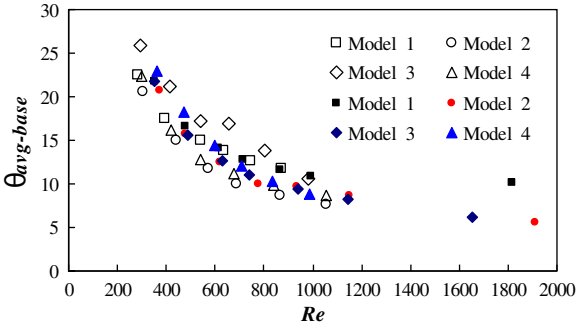

Fig. 7. Dimensionless average plate base temperature (°C) versus Reynolds number for heater set temperatures of 400 °C (*solid symbols*) and of 300 °C (*open symbols*).

which enhances mixing and thus, the heat transfer rate. The turbulence is enhanced by means of increasing the shear production of turbulence which is the product of Reynolds stress and mean velocity gradients. No heat transfer enhancement in models 2, 3, and 4 indicates that under given conditions, increased shear production of turbulence does not influence the wall heat transfer. This issue was further investigated in detail. Since the results were identical for all models, the base model (i.e. Model 1) was considered for further investigations. As shown previously, the plate base and plate tip temperatures were calculated for all models and cases. In solar collectors as in the present setup, the incident heat flux to the pipe is not uniform. The heat flux into the pipe is due to radiation heat transfer from the upper portion of the pipe exposed directly to the radiation and due to the conduction heat transfer

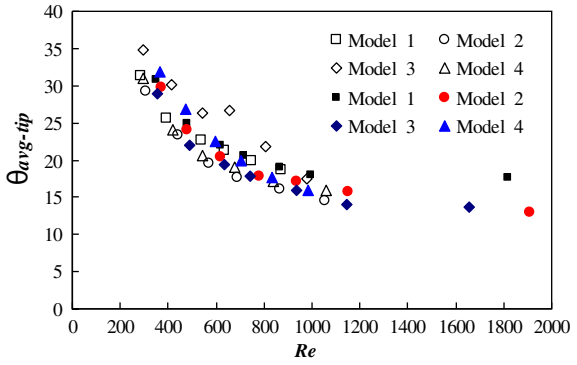

Fig. 8. Dimensionless average plate tip temperature (°C) versus Reynolds number for heater set temperatures of 400 °C (*solid symbols*) and of 300 °C (*open symbols*).

from the plate base. Thus, the temperature distribution on the pipe at any particular cross-section is not uniform. The average pipe wall temperature was required for further analysis; however, it could not be estimated just from the plate base temperature. Therefore, for the base model (Model 1) which was used for detailed analysis, the temperature at the pipe outer wall was also measured on the upper side that was exposed to the radiant heater and the lower side that was not exposed to direct radiation, at three axial locations (see Fig. 2 for the position of thermocouples for these measurements). The average pipe wall temperature was obtained by averaging the upper and lower pipe wall temperatures. The average pipe wall and average fluid temperatures for Model 1 are plotted in dimensionless form in Fig. 9 versus the Reynolds number for T_{ph} equal to 400 °C. The plot shows that both the pipe wall temperature and average fluid temperature increased with a decrease in the flow rate. A similar trend was also observed for T_{ph} equal to 300 °C [20]. The plot also shows that the difference between the normalized average wall and average fluid temperatures is approximately 10 °C. In the actual units, this temperature difference is more than 20 °C. At a given cross-section of the pipe, large temperature gradients (i.e. 20 °C over a distance of approximately 7 mm) cause a large variation in the fluid density and thus, strong flow stratification.

When a solar collector is heated by radiation, the flow pattern is more complicated than that of a uniformly heated individual pipe since the upper surface of the tube is subjected to the direct radiation and it is warmer than the lower surfaces. The base of the collector plate also creates localized regions of high temperature. As a result, a stably stratified layer of light and warm fluid is maintained near the top of the pipe which does not undergoes significant mixing with the colder core fluid. The relatively warmer

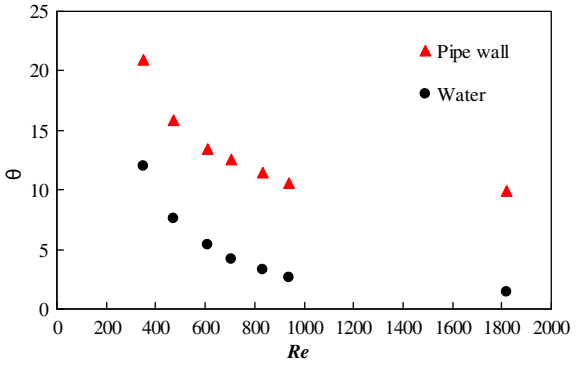

Fig. 9. Dimensionless average pipe wall and average water temperatures for model 1 versus Reynolds number for heater set temperature of 400 °C.

fluid near the base of the collector plate and the bottom of the pipe induces convective motions in the lower section of the tube.

In a pure forced convection system, the shear-produced turbulence influences the heat transfer coefficient and hence the wall heat transfer. However, if the flow stratification increases, the buoyancy effect becomes significant, which influences shear-produced turbulence and heat transfer. One important dimensionless parameter that quantifies the influence of buoyancy is the Grashof number (Gr), defined as the ratio of the buoyancy forces to the viscous forces. Gr is a measure of the intensity of free convection and has a similar role as the Reynolds number in the forced convection. The combined effect of free and forced convection appears, generally, when $Gr/Re^2 \approx 1$. When $Gr/Re^2 \gg 1$ the effect of free convection is dominant and the Nusselt number is a function of Gr and Pr; whereas, for $Gr/Re^2 \ll 1$, forced convection is dominant and the Nusselt number is function of Re and Pr [17,21]. The variation of Grashof number (Gr), which is based on the temperature difference between pipe wall and bulk flow (Eq. (11)), and the modified Grashof number (Gr_q), which is based on the wall heat flux (Eq. (15)) for both T_{ph} values is presented in Fig. 10 versus the Reynolds number. The plot shows that for any Reynolds number, the Gr and Gr_q are in the range of 10^6 and 10^7, respectively. This indicates that under given conditions, free convection is the dominant heat transfer mode. These results also indicate that the free convection is much stronger at lower Reynolds numbers, as expected.

In density stratified flows, the gravity forces that manifest themselves in the buoyancy force form are very important. Richardson number (or the gradient Richardson number) is another parameter that determines the intensity of the free convection relative to the forced convection. Gradient Richardson number is related to the ratio of the buoyancy to inertial forces [22].

The critical value of the gradient Richardson number above which shear flows are linearly stable, is 0.25. However, when $Ri \gg 1$, the stratification is more dominant than the shear forces [23]. The Richardson number is also presented in another form called, the flux Richardson number (Ri_f), which is related to the gradient Richardson number and is defined as the rate of removal of energy by buoyancy forces to the turbulent energy production by shear forces [22]. The critical value of the Ri_f is also 0.25. For $Ri_f > 1$, buoyancy removes energy from the fluid at much higher rate than its production by the shear forces. Therefore, when flux or gradient Richardson number is above unity, the flow is considered to be stably stratified and the turbulence is damped by working against the buoyancy forces and heat transfer is almost entirely due to free convection. Fig. 11 shows the variation of the Ri based on the supplied flux (Eq. (18)) and Ri_q (Eq. (17)) versus the Re, for both T_{ph} values. Results show that for $T_{ph} = 400$ °C, as Re decreased from 1820 to 350, the flux based Richardson number and modified Richardson increased from approximately 14 to 5440 and 7 to 330,

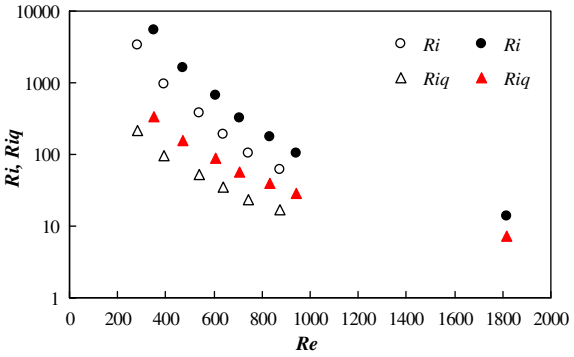

Fig. 11. Variation of Ri and Ri_q numbers versus Re for heater set temperatures of 400 °C (*solid symbols*) and 300 °C (*open symbols*).

respectively. For $T_{ph} = 300$ °C, when Re decreased from 875 to 280, the values of Ri and Ri_q increased from approximately 60 to 3400 and 17 to 212, respectively. These results show that the Richardson numbers are significantly higher than the critical value of 0.25 which indicates that for the present conditions, the flows are stably stratified with very high degree of flow stability thus, most of turbulence produced by the shear is utilized or damped by working against the buoyancy forces and hence does not play a significant role in heat transfer. Increase in stability for stratified flows reduces the turbulent intensity. That is why, all applied passive methods, based on the shear production are ineffective in augmenting heat transfer to the fluid.

Another important parameter, which is a measure of the generation and perturbation of free convection, is the Rayleigh number (Ra). Ra is a measure of the relative amount of viscous and buoyant forces. The onset of free convection occurs at a critical Rayleigh number of 1708. Beyond this critical value, the flow becomes unstable and for $Ra > 10^5$ transition to turbulence begins. For $Ra > 10^6$–10^7, the flow becomes fully turbulent [24]. The structure of this turbulence is fundamentally different from that generated by the shear flow. The Rayleigh number (Eq. (13)) and modified Rayleigh number (Eq. (16)) for both T_{ph} values are plotted in Fig. 12 versus the Re. The results show that, in the present study, values of Ra and Ra_q are in the range of 10^7–10^8. Such large values indicate that flow inside the tube is thermally turbulent and free convection is the dominant heat transfer mode.

Mixed convection (i.e. the combination of laminar free and forced convection) in horizontal straight tubes have been extensively studied over the past few decades and several correlations have been developed for heat transfer in mixed convection regime (e.g. [25–27,28,29]). Most of the previous experimental studies on

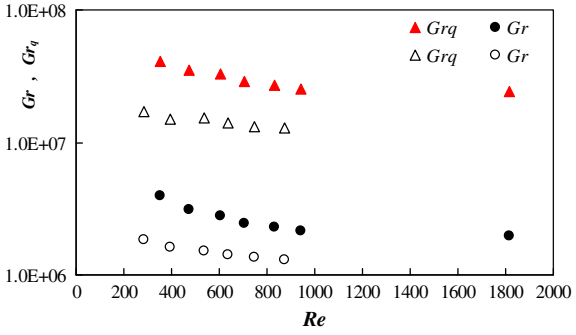

Fig. 10. Variation of Gr and Gr_q numbers versus Re for heater set temperatures of 400 °C (*solid symbols*) and 300 °C (*open symbols*).

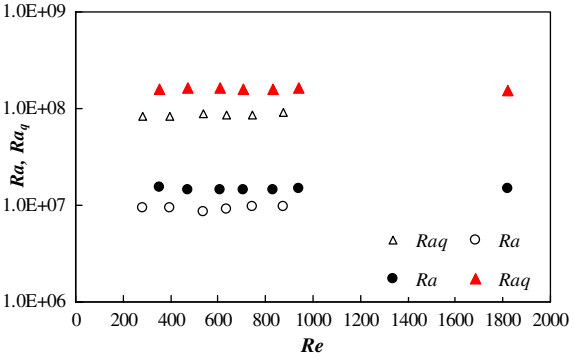

Fig. 12. Variation of Ra and Ra_q numbers versus Re for heater set temperatures of 400 °C (*solid symbols*) and 300 °C (*open symbols*).

mixed convection, however, used very simple geometry, e.g. straight horizontal tube. Similarly, the method of heat transfer to the system was also simple, e.g. either the heat source surrounded uniformly all around the pipe or the tested section was heated from below (in case of rectangular ducts). As a result, they observed good agreements between their measurements and reported correlations. Few studies have reported mixed convection in solar collector geometry; however, the mode of heat transfer or in other words, the thermal boundary conditions were significantly different from the real application of the solar collector. For example, Iqbal [9] imposed a uniform heat flux boundary condition through electrical wires coiled around an inclined tube. The experimental model of Barozzi et al. [10] was a plate-and-tube geometry; however, they inserted equally spaced electrical wires into the two plates to provide heat flux. Therefore, due to the dissimilar geometry, boundary condition, and heat transfer modes, the results from the previous studies (either heat enhancement methods or mixed convection inside horizontal tubes) cannot be applied directly to solar collectors and hence, to the results in the present study. Furthermore, in the present case, not only the heat source, heating direction, and module's geometry were dissimilar from the previous studies but also the ranges of *Ra* and *Gr* in the present study were significantly higher than the limits of correlations reported in most of those studies, such as famous correlations suggested by [18] and [30]. Therefore, the correlations developed for mixed convection in the conventional setup cannot be used to validate our data. The values of the average Nusselt number obtained from the experimental data using Eqs. (7) and (8) are plotted versus the Rayleigh and modified Rayleigh numbers in Fig. 13(a) and (b) for T_{ph} values of 400 and 300 °C, respectively. Siegwarth et al. [31] presented a correlation for the Nusselt number in fully developed mixed convection flow in horizontal tube with uniform heat flux. Barozzi et al. [10] expressed the correlation of Siegwarth et al. [31] in the form of modified Rayleigh number as

$$Nu = 0.629 Ra_q^{1/5} \tag{19}$$

The values of Nusselt number predicted from Eq. (19) for the given cases are also plotted in Fig. 13 for comparison. The results as expected showed that the correlation for a uniform heat flux around the tube overestimates the Nusselt number by more than a factor of two for all cases. In the experimental study of [10], the experimental model was similar to our study (i.e. flat-plate collector); however, heat was imposed to the models by means of electrical elements longitudinally inserted inside the absorber plate to provide uniform heat flux. They reported values of local Nusselt numbers, in the range of 5–10 for various flow rates and heat fluxes, which are lower than the present values. Catton [32] presented correlations for free convection inside rectangular cavities where two sides of the rectangular cavity are insulated and two other sides are kept at different temperatures, i.e. heated and cooled surfaces. Despite of different geometries, there is some similarity in thermal boundary conditions between his model and the present setup. For *Ra* between 10^6 and 10^9, and *Pr* between 1 and 20, this correlation is presented as

$$\overline{Nu}_L = 0.046 Ra^{1/3} \tag{20}$$

The values of Nusselt number predicted from this correlation are also presented in Fig. 13. The results show very good agreement with the present data. A good agreement with the correlation developed for different heat fluxes at the top and bottom walls in a rectangular geometry [32] and significant overestimation with the correlation developed for constant heat flux but circular geometry [31] indicate that the adaptability of a correlation to the given setup is more sensitive to the thermal boundary conditions than the flow geometry. The trends in Fig. 13 show that a correlation of the form presented in Eq. (20) fits our data properly. However, more detailed experiments with a larger range of experimental conditions are required to confirm the present trend and establish a comprehensive correlation for the mixed convection in flat-plate solar collectors.

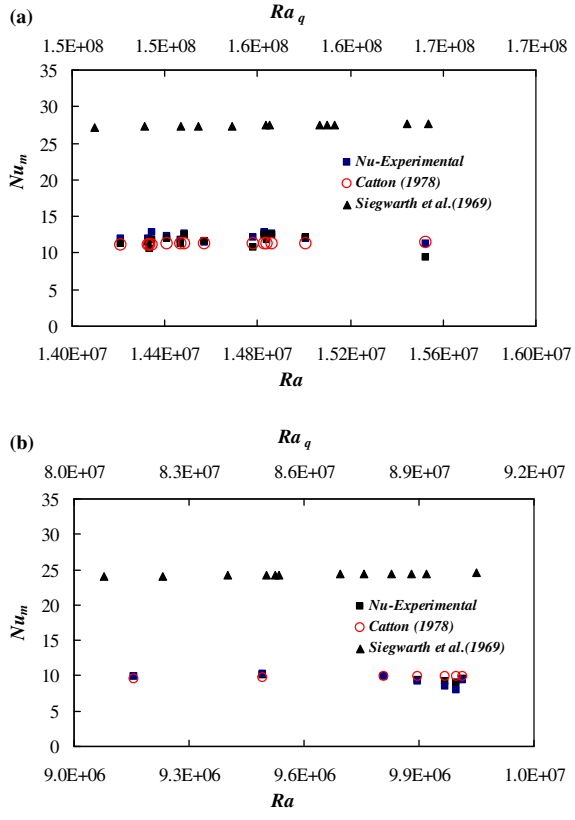

Fig. 13. Comparison of the average *Nu* obtained in the present study with that obtained from the correlations of Siegwarth et al. [31] and Catton [32] for heater set temperatures of (a) 400 °C and (b) 300 °C.

5. Conclusion

An experimental study was conducted to investigate the impact of heat enhancement devices on the thermal performance of a solar collector. Four different models of solar collectors were tested in a laboratory setup with different passive heat transfer enhancement devices. The comparison showed that the heat enhancement devices are ineffective in enhancing heat transfer rate in the studied range and geometry. A detailed investigation of the observed trend showed significantly high values of Grashof, Richardson, and Rayleigh numbers indicating that the heat transfer mode in the solar collector is mixed convection with the predominance of free convection. The values of Richardson number are one to four orders of magnitude higher that the critical value of 0.25 implying that the flow is stably stratified causing a significant damping of shear-produced turbulence. It is argued that most of the turbulence produced and enhanced by heat enhancement devices is utilized or damped by working against the buoyancy forces and hence does not play a significant role in heat transfer. Hence, it is concluded that the applied passive methods based on the enhancement of shear-produced turbulence are ineffective in augmenting heat transfer to the collector fluid in flat-plate solar collectors. It was also observed that due to the difference in geometry and thermal boundary conditions, the correlations developed for mixed convection in the conventional setup overestimate the Nusselt number by more than a factor of two. The results also indicate that

the adaptability of a correlation to the given setup is more sensitive to the thermal boundary conditions than the flow geometry. In solar collectors, where the flow rates are low and the temperature difference between the pipe wall and bulk fluid is significantly high, buoyant forces coupled with the axial flow create a three-dimensional complex fluid motion where conventional heat enhancement methods does not work. Detailed investigation of flow and thermal behavior in solar collectors is therefore necessary to understand this complex dynamics that would lead to the development of effective ways to improve the thermal performance of solar collectors.

References

[1] J.A. Duffie, W.A. Beckman, Solar Engineering of the Thermal Processes, second ed., Wiley, New York, 1991.
[2] E. Smithberg, F. Landis, Friction and forced convection heat-transfer characteristics in tube with twisted tape swirl generators, Trans. ASME, Ser. C, J. Heat Transfer 86 (1) (1964) 39–49.
[3] E.G. Narezhnyy, A.V. Sudarev, Local heat transfer in air flowing in tubes with a turbulence promoter at the inlet, Int. J. Heat Mass Transfer 2–3 (1971) 62–66.
[4] S.W. Hong, A.E. Bergles, Augmentation of laminar flow heat transfer in tubes by means of twisted-tape insert, Trans. ASME, Ser. C, J. Heat Transfer 98 (1) (1976) 251–256.
[5] G.H. Junkhan, A.E. Bergles, V. Nirmalan, T. Ravigururajan, Investigation of turbulators for fire tube boilers, Trans. ASME, J. Heat Transfer 107 (2) (1985) 354–360.
[6] C. Yildiz, Y. Bicer, D. Pehlivan, Effect of twisted strips on heat transfer and pressure drop in heat exchangers, Energy Convers. Manage. 39 (3/4) (1998) 331–336.
[7] A. Durmuş, A. Durmuş, M. Esen, Investigation of heat transfer and pressure drop in a concentric heat exchanger with snail entrance, Appl. Therm. Eng. 22 (2002) 321–332.
[8] P. Promvonge, S. Eiamsa-ard, Heat transfer enhancement in a tube with combined conical-nozzle inserts and swirl generator, Energy Convers. Manage. 47 (2006) 2867–2882.
[9] M. Iqbal, Free-convection effects inside tubes of flat-plate solar collectors, Solar Energy 10 (4) (1966) 207–211.
[10] G.S. Barozzi, E. Zanchini, M. Mariotti, Experimental investigation of combined forced and free convection in horizontal and inclined tubes, MECCANICA 20 (1985) 18–27.
[11] M. Ouzzane, N. Galanis, Numerical analysis of mixed convection in inclined tubes with external longitudinal fins, Solar Energy 71 (3) (2001) 199–211.
[12] ASTM B88-99, Standard specification for seamless copper water tube, ASTM standards.
[13] A. Hobbi, K. Siddiqui, Optimal design of a forced circulation solar water heating system for a residential unit in cold climate using TRNSYS, Solar Energy 83 (2009) 700–714.
[14] M.A. Habib, A.A.A. Negm, Laminar mixed convection in horizontal concentric annuli with non-uniform circumferential heating, Heat Mass Transfer 37 (2001) 427–435.
[15] F.C. Chou, W.Y. Lien, Effect of wall heat conduction on laminar mixed convection in the thermal entrance region of horizontal rectangular channel, Wärmeund Stoffübertragung 26 (1991) 121–127.
[16] S. Piva, G.S. Barozzi, M.W. Collins, Combined convection and wall conduction effects in laminar pipe flow: numerical predictions and experimental validation under uniform wall heating, Heat Mass Transfer 30 (1995) 401–409.
[17] F.P. Incropera, D.P. De Witt, TH.L. Bergman, A.S. Lavine, Fundamentals of Heat and Mass Transfer, sixth ed., Wiley, New York, 2007.
[18] S.M. Morcos, A.E. Bergles, Experimental investigation of combined forced and free laminar convection in horizontal tubes, J. Heat Transfer, Trans. ASME 97 (1975) 212–219.
[19] C. Bonnefoi, C. Abid, M. Medale, F. Papini, Poiseuille–Benard instability in a horizontal rectangular duct water flow, Int. J. Therm. Sci. 43 (2004) 791–796.
[20] A. Hobbi, Design of solar water heating systems for cold climate and study of heat transfer enhancement devices in flat-plate solar collectors, M.A.Sc. Thesis, Concordia University, Montreal, Canada, 2007.
[21] F.M. White, Viscous Fluid Flow, second ed., McGraw-Hill, New York, 1991.
[22] J.S. Turner, Buoyancy Effects in Fluids, Cambridge University Press, UK, 1973.
[23] A.J. Majda, M. Shefter, The instability of stratified flow at large Richardson numbers, Appl. Math. 95 (1998) 7850–7853.
[24] F.H. Busse, Non-linear properties of thermal convection, Rep. Prog. Phys. 41 (1978).
[25] A.J. Ede, The heat transfer coefficient for flow in a pipe, Int. J. Heat Mass Transfer 4 (1961) 105–110.
[26] S.T. McComas, E.R.G. Eckert, Combined free and force convection in a horizontal circular tube, J. Heat Transfer, Trans. ASME 88 (1966) 147–153.
[27] Y. Mori, K. Futagami, Forced convection heat transfer uniformly heated horizontal tubes, Int. J. Heat Mass Transfer 10 (1967) 1801–1813.
[28] G.N. Faris, R. Viskanta, An analysis of laminar combined forced and free convection heat transfer in a horizontal tube, Int. J. Heat Mass Transfer 12 (1969) 1295–1309.
[29] P.H. Newell, A.E. Bergles, Analysis of combined free and forced convection for fully developed laminar flow in horizontal tubes, J. Heat Transfer, Trans. ASME 92 (1970) 83–89.
[30] A.R. Brown, M.A. Thomas, Combined free and forced convection heat transfer for laminar flow in horizontal tubes, J. Mech. Eng. Sci. 7 (4) (1965) 440–448.
[31] D.P. Siegwarth, R.D. Miksell, T.C. Readal, T.J. Hanratty, Effect of secondary flow on the temperature filed and primary flow in a heated horizontal tube, Int. J. Heat Mass Transfer 12 (1969) 1535–1552.
[32] I. Catton, Natural convection in enclosures, in: Proc. 6th Int. Heat Transfer Conference, vol. 6, Toronto, Canada, 1978, pp. 13–31.